JACS
JOURNAL OF THE AMERICAN CHEMICAL SOCIETY
Article
pubs.acs.org/JACS

Deamidation of Asparagine to Aspartate Destabilizes Cu, Zn Superoxide Dismutase, Accelerates Fibrillization, and Mirrors ALS-Linked Mutations

Yunhua Shi,[†] Nicholas R. Rhodes,[†] Alireza Abdolvahabi,[†] Taylor Kohn,[†] Nathan P. Cook,[‡] Angel A. Marti,[‡,§] and Bryan F. Shaw*[,†]

[†]Department of Chemistry and Biochemistry, Baylor University, Waco, Texas 76706, United States
[‡]Department of Chemistry and [§]Department of Bioengineering, Rice University, Houston, Texas 77005, United States

Supporting Information

ABSTRACT: The reactivity of asparagine residues in Cu, Zn superoxide dismutase (SOD1) to deamidate to aspartate remains uncharacterized; its occurrence in SOD1 has not been investigated, and the biophysical effects of deamidation on SOD1 are unknown. Deamidation is, nonetheless, chemically equivalent to Asn-to-Asp missense mutations in SOD1 that cause amyotrophic lateral sclerosis (ALS). This study utilized computational methods to identify three asparagine residues in wild-type (WT) SOD1 (i.e., N26, N131, and N139) that are predicted to undergo significant deamidation (i.e., to >20%) on time scales comparable to the long lifetime (>1 year) of SOD1 in large motor neurons. Site-directed mutagenesis was used to successively substitute these asparagines with aspartate (to mimic deamidation) according to their predicted deamidation rate, yielding: N26D, N26D/N131D, and N26D/N131D/N139D SOD1. Differential scanning calorimetry demonstrated that the thermostability of N26D/N131D/N139D SOD1 is lower than WT SOD1 by ~2−8 °C (depending upon the state of metalation) and <3 °C lower than the ALS mutant N139D SOD1. The triply deamidated analog also aggregated into amyloid fibrils faster than WT SOD1 by ~2-fold ($p < 0.008$**) and at a rate identical to ALS mutant N139D SOD1 ($p > 0.2$). A total of 534 separate amyloid assays were performed to generate statistically significant comparisons of aggregation rates among WT and N/D SOD1 proteins. Capillary electrophoresis and mass spectrometry demonstrated that ~23% of N26 is deamidated to aspartate (iso-aspartate was undetectable) in a preparation of WT human SOD1 (isolated from erythrocytes) that has been used for decades by researchers as an analytical standard. The deamidation of asparagine—an analytically elusive, sub-Dalton modification—represents a plausible and overlooked mechanism by which WT SOD1 is converted to a neurotoxic isoform that has a similar structure, instability, and aggregation propensity as ALS mutant N139D SOD1.

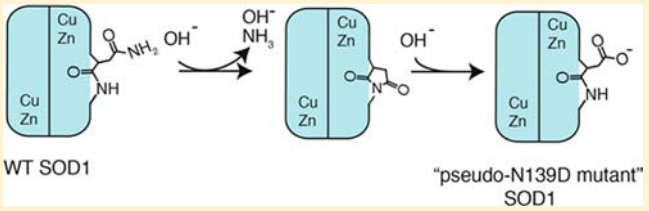

INTRODUCTION

The rate at which asparagine residues in folded proteins deamidate (non-enzymatically) to aspartic acid (Figure 1) is generally slow at neutral pH and can vary from days to decades depending upon the primary and three-dimensional structure of the protein.[1−4] For example, the presence of glycine and other small, unbranched amino acids at the C-terminal flank of an asparagine will generally increase the rate of deamidation, whereas C-terminal flanking by bulkier branched residues (and proline) will diminish the rate of deamidation. The folding of proteins also generally slows the rate of deamidation by reducing solvent accessibility and increasing conformational rigidity and intramolecular H-bonding.[1] The non-enzymatic deamidation of asparagine in folded proteins is commonly associated with long-lived proteins,[5−7] and its perennial occurrence in aqueous environments has led to the hypothesis that the reaction functions as a "molecular clock" by which organisms can genetically control the amino acid sequence of proteins as a function of time.[2,4,8]

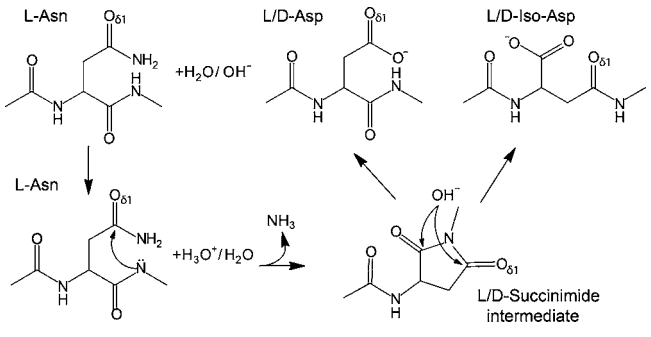

Figure 1. Chemical mechanism of spontaneous (non-enzymatic) asparagine deamidation. The reaction can produce different products, including the stereoisomers of aspartate or iso-aspartate and cleavage products (which are not shown for clarity).

Received: July 29, 2013
Published: September 25, 2013

   dx.doi.org/10.1021/ja407801x | J. Am. Chem. Soc. 2013, 135, 15897−15908

We suspect that the spontaneous deamidation of asparagine to aspartate might be intrinsically toxic to motor neurons, and represent more of a "ticking time bomb", because it is chemically indistinguishable from toxic Asn-to-Asp missense mutations. For example, the N86D and N139D missense mutations in the gene encoding Cu, Zn, superoxide dismutase (SOD1)[9] cause familial forms of amyotrophic lateral sclerosis (ALS),[10] as do the more recently discovered ALS-linked missense mutations N378D and N390D in the TARDBP gene encoding the transactive response DNA binding protein-43 (TDP-43).[11−14] It is reasonable to suspect that the spontaneous deamidation of asparagine might occur to SOD1 and TDP-43 within motor neurons (more so than in other cell types) because these proteins undergo axonal transport.[14,15] Axonal transport in motor neurons can involve distances that exceed one meter and durations that exceed one year, e.g., the SC-b (slow component-b) axonal transport[16] of SOD1 proceeds at a rate of 2−8 mm/day.[15] In contrast, a protein such as SOD1 would be, we hypothesize, less susceptible to deamidation in other cell types where its lifetime is typically shorter by a factor of 100 (e.g., the SOD1 protein has a measured lifetime of <100 h when overexpressed in cultured HEK or COS cells).[17]

To date, more than 160 different mutations in the gene encoding SOD1 have been linked to familial forms of ALS. Most of these mutations result in single amino acid substitutions that induce toxicity by (presumably) increasing the rate of self-assembly of SOD1 into fibrillar oligomers that are rich in β-sheet structure. The aggregation of the wild-type (WT) SOD1 protein is now also hypothesized to cause sporadic forms of ALS.[18,19] A growing list of post-translational chemical modifications (non-proteolytic) have been detected (or are at least hypothesized) to occur to SOD1 *in vivo* or *in vitro*,[19−28] and several of these modifications are hypothesized to convert the WT SOD1 protein into a neurotoxic isoform that self-assembles into fibrillar structures at a rate or form reminiscent of ALS mutant SOD1.[19,20]

The deamidation of asparagine to aspartate is unique among post-translational modifications that are suspected to occur to SOD1 and be involved in ALS, both in its potential relevance to ALS and the urgency with which we must characterize its occurrence and biophysical effects upon SOD1 because: (i) deamidation is the only known modification that represents a post-translational "mutation" that is chemically equivalent to neurotoxic mutations; (ii) deamidation (Δmass = +0.984 Da) is an analytically elusive modification that, if occurring *in vivo* (or even *in vitro*), has likely been undetected in prior mass spectrometric analyses of SOD1; and (iii) the slow kinetics of deamidation suggest that the reaction will occur selectively to SOD1 expressed in motor neurons. In fact, it appears obligatory to conclude, *a priori*, that asparagine deamidation at N86 and N139 in SOD1 produces an SOD1 polypeptide that is just as intrinsically toxic to motor neurons as the polypeptide that results from the chemically synonymous N86D and N139D missense mutations to the SOD1 gene. Such a conclusion cannot be rationally made, *a priori*, about other types of post-translational modifications to SOD1.

The deamidation of asparagine in WT SOD1 has not been explicitly investigated (or even cited in the literature) as a modification that might convert WT SOD1 into a neurotoxic isoform. Moreover, asparagine deamidation has not even been reported to occur to full-length human SOD1 *in vivo* or *in vitro*, within (or beyond) the context of ALS. Nevertheless, the perfunctory detection of a subpopulation of deamidated SOD1, followed by the verification that deamidation occurred *in vivo* (and not during sample preparation) are both complicated by the small change in molecular mass associated with deamidation and by the difficulty in distinguishing whether deamidation occurred *in vivo* or occurred artifactually during sample preparations that will increase the solvent accessibility and conformational flexibility of Asn residues (e.g., proteolysis with trypsin or denaturation with urea).[29] Furthermore, the type of mass analyzers (i.e., time-of-flight, quadrupole, or ion-trap) and proteolysis protocols that were used in most of the previous mass spectrometric analyses of human SOD1 from neural tissue, e.g., the study by Shaw et al.,[30] would not have been able to detect subpopulations of full-length SOD1 proteins bearing sub-Dalton modifications.[26,31−33] Detecting subpopulations of SOD1 with sub-Dalton modifications is even difficult with Fourier transform ion cyclotron resonance-MS instruments (because of naturally occurring carbon isotopes), as shown in a recent study that distinguished subpopulations of Cu-SOD1 (gas phase) from Zn-SOD1 (Δmass Cu:Zn = 1.84 Da).[34]

In this paper, we show (computationally) that several asparagine residues in SOD1 undergo significant deamidation on time-scales comparable to the SC-b axonal transport of SOD1 in a motor neuron. We also measured the biophysical effects of deamidation of multiple asparagines (to aspartate) in WT SOD1. The results demonstrate that the successive deamidation of multiple asparagines has similar effects on the structure, thermostability, and rate of self-assembly of SOD1 into amyloid as the ALS-linked missense mutation N139D. To illustrate the elusiveness of deamidation and begin to determine its occurrence *in vivo*, we show that asparagine is deamidated to aspartate (not iso-aspartate) and has gone undetected in a common commercial source of human SOD1 (isolated from human blood) that has been utilized for >30 years as a standard in the electrophoretic, immunohistochemical, and enzymological studies of SOD1 biochemistry and reactive oxygen species.

RESULTS AND DISCUSSION

The SOD1 protein is expected to endure a lifetime on the order of 1.4 years when traversing an axon that is 1 m in length at a rate of 2 mm/day.[15] The lifetime of SOD1 that is localized to axons might also be increased by deficits in axonal transport, which can precede the death of motor neurons and can be associated with ALS.[35] With these time-scales in mind, we used an algorithm previously developed by Robinson and Robinson[4] to predict the rate of deamidation of all seven Asn residues in a subunit of homodimeric WT holo-SOD1 (at pH 7.4, 37 °C). The calculations were performed upon an NMR solution structure of WT holo-SOD1 (PDB entry: 1L3N); the details of the algorithm and its use to predict deamidation rates have been reviewed.[1] Briefly, the free energy of activation required to rearrange the Asn side chain (to permit optimal formation of the cyclic succinimide intermediate) is approximated from a parametrized function that accounts for the local primary structure and flexibility of each asparagine (i.e., the local 2° and 3° structure and H-bonding). The location of each Asn residue (and its solvent accessibility) in folded holo-SOD1 is shown in Figure 2A; the secondary structure of each Asn residue in holo-SOD1 is shown in Figure 2B.

The shortest half-life of Asn deamidation in folded, holo-SOD1 was calculated to be $t_{1/2}$ = 71 days for N26 (which is solvent exposed and C-terminally flanked by Gly27), and the longest was $t_{1/2}$ = 48.5 years for N86 (which is buried and C-

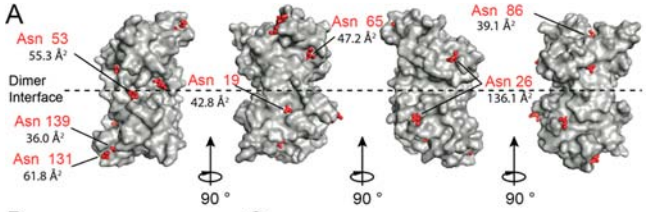

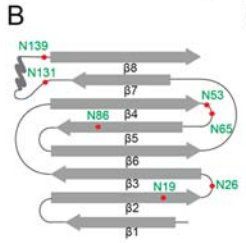

C

Asn	hSOD1 sequence	Predicted half-life, folded holo-SOD1 (Days)	Peptide analog	Measured half-life, peptide analog (Days)
19	IINFE	11650	GINFG	61.5
26	ESNGP	71	GSNGG	0.96
53	GDNTA	17127	GDNTG	52.4
65	HFNPL	2725	GFNPG	7990
86	LGNVT	17705	GGNVG	224
131	GGNEE	351	GGNEG	73.9
139	TGNAG	1317	GGNAG	21.1

Figure 2. (A) Three-dimensional structure of human WT SOD1 (PDB: 1L3N) with its seven Asn side chains highlighted in red; the solvent accessible surface area of each Asn is listed (as approximated from the rolling sphere method, using Accelrys Discovery Studio). (B) Secondary structure map of WT holo-SOD1. (C) Calculated (theoretical) half-lives of deamidation for all seven Asn residues in folded holo-SOD1 at pH 7.4, 37 °C. Half-lives were calculated by analysis of the NMR-derived solution structure of WT holo-SOD1 (PDB entry: 1L3N) with an algorithm developed by Robinson and Robinson.[4] Also shown: the previously measured half-lives of deamidation of seven different pentapeptides[1] (at pH 7.4, 37 °C) that have homologous neighboring residues ($n + 1$ and $n - 1$) to the seven Asn residues in SOD1.

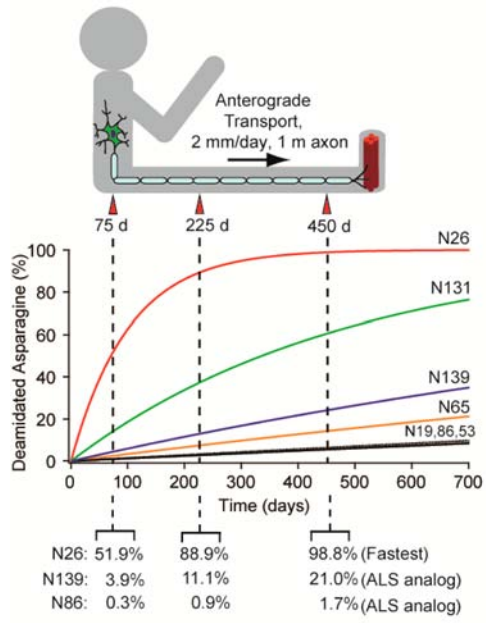

Figure 3. Comparison of the predicted extent of deamidation of holo-SOD1 (as estimated by an algorithm developed by Robinson and Robinson)[4] with the rate of anterograde SC-b axonal transport of SOD1 (at 2 mm/day) in a motor neuron that is 1 m in length.

terminally flanked by Val87) (Figure 2C). The half-life of N139 was predicted to be $t_{1/2}$ = 3.6 years in folded holo-SOD1. Asparagine residues in holo-SOD1 were predicted to undergo deamidation in the following order: N26 > N131 > N139 > N65 > N19 > N53 > N86. We did not attempt to predict the effect of the deamidation of one Asn residue on the rate of deamidation of a separate Asn residue. In order to estimate the intrinsic half-life of Asn residues in disordered SOD1 or peptide fragments of SOD1, such as those that might be generated during proteolysis (*in vitro*, prior to MS/MS sequencing), we searched published libraries of measured rates of deamidation for ∼400 pentapeptides[1] and found 7 pentapeptides with Asn residues that have identical $n + 1$ and $n - 1$ residues to the 7 Asn in SOD1. Notably, $t_{1/2}$ = 0.96 days for the N26 analog pentapeptide, and $t_{1/2}$ = 21.1 days for the N139 analog, at pH 7.4–7.5, 37 °C (Figure 2C).

The predicted rates of Asn deamidation in holo-SOD1 were compared with its timespan of anterograde SC-b axonal transport through an axon measuring 1 m in length (Figure 3). After ∼450 days, 99% of holo-SOD1 polypeptides were predicted to have undergone deamidation at N26; 55% at N131; 21% at N139, and 2% at N86 (Figure 3). These approximations led us to hypothesize that the deamidation of N26, N131, and N139 might occur at significant levels (i.e., >20%) in SOD1 proteins that traverse long distances during axonal transport.

Successive Asn Deamidation Lowers the Thermostability of WT SOD1. The conformational stability of ALS-linked mutant SOD1 proteins has been shown to correlate negatively with their aggregation propensity and positively with the life-span of ALS patients.[36] In order to determine the effects of successive deamidation on the conformational stability (and other biophysical properties) of SOD1, we used site-directed mutagenesis to introduce the following compounded Asn-to-Asp substitutions into WT SOD1: N26D, N26D/N131D, and N26D/N131D/N139D. The use of Asn-to-Asp missense mutations to mimic deamidation allowed us to: (i) generate pure solutions of "deamidated" SOD1, (ii) control the site of "deamidation", and (iii) generate the deamidated analogs quickly (instead of performing the reaction manually over the course of, presumably, several months under reducing conditions).

An analysis of each recombinantly expressed and purified N/D SOD1 mutant protein (in the demetalated apo state) with circular dichroism and amide hydrogen–deuterium exchange (as measured by mass spectrometry) suggested that the compounded deamidation of N26, N131, and N139 does not significantly affect the three-dimensional structure of apo-SOD1 (Figure 4B–D). All apo-SOD1 proteins retained between 25 and 35 unexchanged hydrogens after 60 min in D_2O, however, a one-way ANOVA test (analysis of variance) of each set of 21 measurements (for each protein) showed no statistically significant difference between the rates of H/D exchange for any of the apo-SOD1 proteins studied at either 5 or 60 min, i.e., $p > 0.05$ (Figure 4C).

In order to demonstrate further that WT apo-SOD1, N139D apo-SOD1, and the triply deamidated analog of apo-SOD1 exhibited similar rates of amide H/D exchange, we mixed the WT, N139D, and N26D/N131D/N139D apo-proteins into a single solution and simultaneously measured their mass in D_2O after 60 min (Figure 4D). The width of the molecular ions for this mixture (i.e., ∼ 20.4 Da) was nearly indistinguishable from the width of the molecular ions of the pure N26D/N131D/N139D apo-SOD1 protein after 60 min in D_2O (i.e., ∼19.5 Da). The small increase in width (0.9 Da) observed for the mixture is likely due to the small variance in the intrinsic molecular weight of the three proteins before H/D exchange (Figure 4D). It is important to point out that increasing the net negative charge of proteins—by only a single unit—can reduce

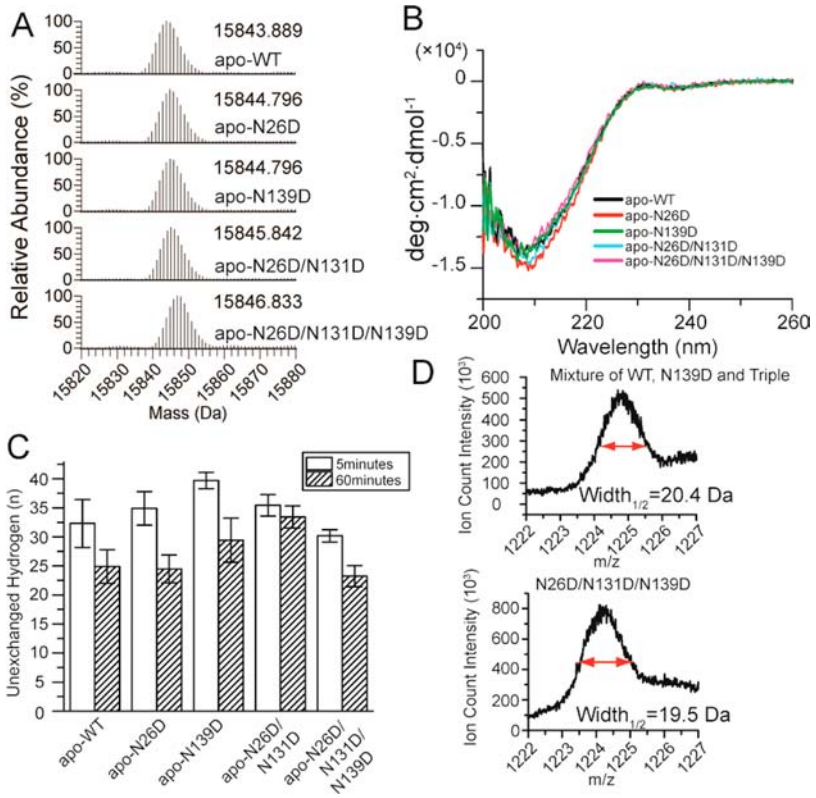

Figure 4. Biophysical effects of successive deamidation of N26, N131, N139 in apo-SOD1 (as modeled by N/D substitutions). (A) Electrospray ionization mass spectra and (B) circular dichroism spectra (at pH 7.4, ~ 22 °C) of N26D, N26D/N131D, and N26D/N131D/N139D apo-SOD1. (C) Solution structure of deamidated analogs is similar, as measured by amide H/D exchange and mass spectrometry (at pD 7.4, ~ 22 °C). Error bars represent standard deviation of 21 replicate measurements (i.e., 7 replicate H/D experiments, measured in triplicate). D) Width of +13 ion of a mixture of WT, N139D, and N26D/N131D/N139D apo-SOD1 after 60 min in D_2O is similar to width of +13 ion of pure apo-SOD1 protein (here, N26D/N131D/N139D apo-SOD1) showing that deamidation does not affect the rate of amide H/D exchange of apo-SOD1.

the rate of amide H/D exchange of that protein at pH > 4 (by either lowering the local concentration of hydroxide catalyst or increasing the free energy of activation of the anionic −N:− intermediate that forms during base-catalyzed amide H/D exchange).[37] These electrostatic (not structural) effects, if occurring from the addition of a single unit of negative charge with each N/D substitution, would likely manifest in reductions in the global rate of exchange of only 1−3 hydrogen ions after 5 or 60 min (which is within our experimental error). Nevertheless, the similarities in rates of amide H/D exchange (and likely, structure) are not surprising when considering that N131 and N139 are located in loop VII, which is intrinsically disordered prior to the coordination of metal ions[38] and the R group of N26 located in loop II is exposed to solvent (Figure 2A,B). All apo-SOD1 proteins in this study were demetalated to contain <0.05 equiv of either copper or zinc per dimer, according to ICP-MS (Table S1).

Each successive N/D substitution lowered the melting temperature (T_m) of apo-SOD1 by <1 °C per substitution (i.e., per deamidation), as measured by differential scanning calorimetry (DSC) (Figure 5A, Table S1). The T_m of the triple mutant (i.e., N26D/N131D/N139D) apo-SOD1 was similar to the ALS-linked N139D apo-SOD1 (i.e., ΔT_m = 0.24 ± 1.46 °C). The successive N/D mutations had a greater destabilizing effect on remetalated (i.e., Cu_2Zn_2) SOD1 than apo-SOD1. All apo-SOD1 proteins were remetalated to contain between 1.73 and 2.05 Cu^{2+} and 1.70−1.87 Zn^{2+} per dimer, according to ICP-MS (Table S1). The thermograms of remetalated WT SOD1 and each mutant protein exhibited one predominant endothermic transition (in the range 82−88 °C) and two minor transitions (each of which likely represent a unique state of metalation, as previously observed for WT and ALS mutant SOD1).[39] Each of the three transition temperatures of the triple mutant was consistently lower than the ALS mutant N139D protein by ~1−3 °C and lower than the WT SOD1 protein by ~3−8 °C (Figure 5B, Table S1). The most straightforward explanation for why the compounded N26D, N131D, and N139D substitutions had a more destabilizing effect on remetalated SOD1 than apo-SOD1 is because N131 and N139 are located in loop VII, which is intrinsically disordered prior to metal binding.[38] Therefore, the N/D substitutions at positions 131 and 139 cannot significantly destabilize a loop in apo-SOD1 that is already intrinsically disordered. Loop VII does, however, become ordered upon metal binding, and the structuring of this loop in the metalated state, which involves the molecular packing and partial burial of N139 (see solvent accessibility values in Figure 2A), is somehow disfavored by the incorporation of a carboxylic acid. This destabilizing effect could be rationalized on the basis that the partial burial of a negatively charged carboxylic acid will be generally disfavored over the partial burial of a neutral amide and/or the H-bond donor ability of the CO_2^- group is lower than the $CONH_2$ group.

Measuring the Effect of Successive Deamidation on the Rate of Self-Assembly of SOD1 into Amyloid. In spite of its destabilized conformation, the triply deamidated SOD1 analog might aggregate slower than N139D SOD1 or WT SOD1 because it has a higher net negative charge than both

dx.doi.org/10.1021/ja407801x | J. Am. Chem. Soc. 2013, 135, 15897−15908

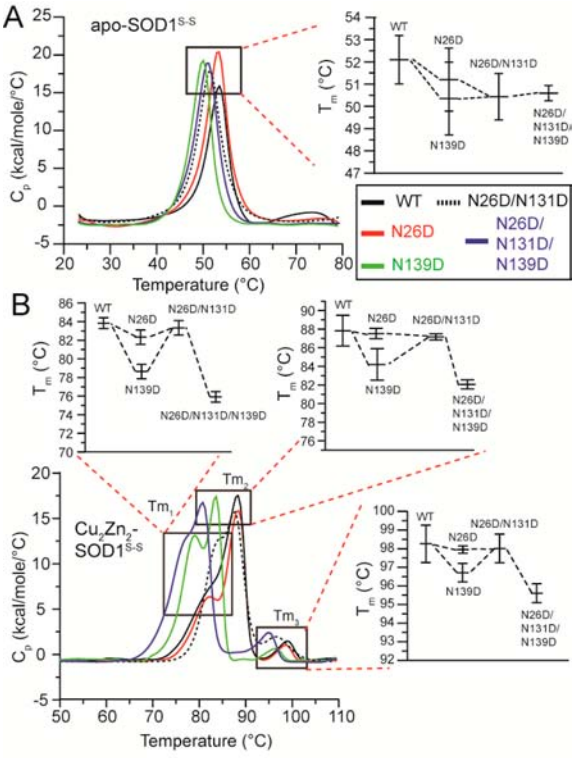

Figure 5. Successive deamidation (as modeled by N/D amino acid substitutions) reduces the thermostability of remetalated SOD1 more than apo-SOD1. (A) Endothermic transitions of N26D, N139D, N26D/N131D, and N26D/N131D/N139D apo-SOD1, with a diagram of resulting T_m values. (B) Endothermic transitions of remetalated N26D, N139D, N26D/N131D, and N26D/N131D/N139D Cu_2Zn_2-SOD1, with diagrams of resulting T_m values. Error bars represent standard error from three separate DSC measurements of each protein.

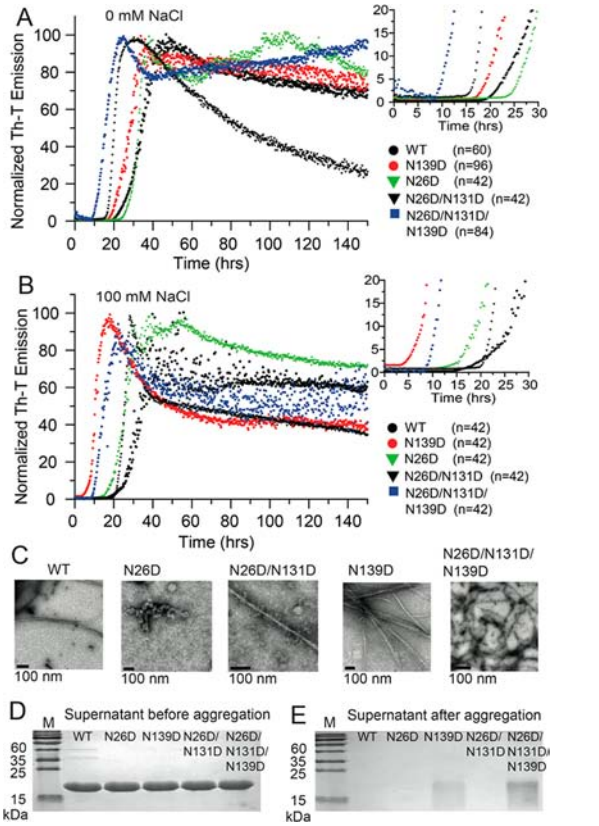

Figure 6. The fibrillization of deamidated analogs of WT apo-SOD1 (disulfide-reduced) into amyloid-like oligomers studied with ThT fluorescence assay and transmission electron microscopy. (A) ThT fluorescence assay for the fibrillization of WT and N/D mutant apo-SOD1 without NaCl; number of replicates, *n*, listed in key. Inset shows magnification of 0−30 h. Only a single longitudinal plot of fluorescence is shown for each protein to indicate sigmoidal increase in ThT fluorescence, i.e., the single plot shown for each protein was randomly chosen and might not correlate with the relative average lag time and inverse propagation constant listed for each protein in Table 1. Longitudinal plots of fluorescence from all replicate experiments (≥42 replicate experiments for each protein) are shown in Figure S2. (B) The same experiment as in part A, but in the presence of 100 mM NaCl. Only a single longitudinal plot of fluorescence is shown for each protein to indicate sigmoidal increase in ThT fluorescence but not to indicate relative average lag times or inverse propagation constants (listed in Table 1) that were calculated from replicate experiments; longitudinal plots of fluorescence from all 42 replicate experiments (for each protein) are shown in Figure S3. (C) Transmission electron micrographs after ThT assay in part A (scale bar = 100 nm). All ThT assays were performed at pH 7.4, 37 °C. (D and E) SDS-PAGE of WT and N/D mutants of apo-SOD1 before aggregation assay (D) and after aggregation assay and centrifugation (E) in 100 mM NaCl.

proteins, which can diminish the rate of aggregation.[40−43] We used a thioflavin-T (ThT) fluorescence assay[44] to quantify the rate of aggregation of N/D mutants and WT SOD1 into amyloid-like fibrils at pH 7.4 (Figure 6). Assays were performed on metal free, disulfide-reduced SOD1 proteins in the absence of NaCl (Figure 6A); Na^+ and Cl^- can screen certain types of attractive or repulsive electrostatic interactions in proteins (e.g., those that occur across a distance that is larger than the Debye screening length, which is ∼1 nm at I = 100 mM, or do not occur across the hydrophobic core of protein that has a low dielectric interior).[45]

Each thioflavin-T amyloid assay was repeated in replicates of 42 to 96 for each protein (depending on protein availability) in the presence or absence of NaCl. Each longitudinal plot of ThT fluorescence generally exhibited a sigmoidal increase in fluorescence (as previously observed for SOD1)[44] that yielded kinetic parameters of fibrillization, i.e., "lag time" and "inverse propagation constant" (Table 1). A graphical illustration of the calculation of lag times and inverse propagation constants from sigmoidal plots of ThT fluorescence is shown in Figure S1. Only a single longitudinal plot of fluorescence from a single replicate experiment is shown for each protein in Figure 6 (to indicate the general sigmoidal shape and not necessarily the average lag time and inverse propagation constant shown in Table 1, that were calculated from dozens of replicate experiments); the intensity of fluorescence was also normalized in these plots. The raw (non-normalized) longitudinal plots of ThT fluorescence for each protein (a total of 534 plots) are included in Supporting Information (Figures S2 and S3; replicate experiments that were carried out in 0 mM NaCl are shown in Figure S2, and experiments in 100 mM NaCl are shown in Figure S3). The terminal reduction in fluorescence that occurred in some of the replicate assays at the end of fibrillization, after reaching a maximum intensity (Figure 6A,B), is an artifact that can be attributed to the adhesion of aggregated SOD1 to the sides of the microplate wells (as inferred from visual inspection); data points within this region were not included in the sigmoidal fit. The fibrillar morphology

dx.doi.org/10.1021/ja407801x | J. Am. Chem. Soc. 2013, 135, 15897−15908

Table 1. Kinetic Parameters of Fibrillization (i.e., lag time and inverse propagation constant) of Deamidated Analogs of WT apo-SOD1 and ALS-Linked N139D apo-SOD1 (at pH 7.4)

SOD1	inverse propagation constant[a] (hr)	*P* value[b]	lag time[a] (hr)	*P* value[b]	*N*[c]	average R^2
0 mM NaCl						
WT	5.3 ± 0.4		26.2 ± 1.5		60	0.98
N139D[d]	3.3 ± 0.1	<0.0001	17.7 ± 1.1	<0.0001	96[e]	0.97
N26D	2.4 ± 0.2	<0.0001	31.2 ± 1.9	0.0430	42	0.99
N26D, N131D	3.5 ± 0.3	0.0010	33.3 ± 2.7	0.0159	42	0.99
N26D, N131D, N139D	3.4 ± 0.3	0.0003	15.7 ± 1.0	<0.0001	84[f]	0.92
100 mM NaCl						
WT	3.5 ± 0.3		18.9 ± 1.2		42	0.97
N139D[g]	2.9 ± 0.2	0.1110	12.9 ± 1.1	0.0006	42[h]	0.97
N26D	3.0 ± 0.3	0.2099	22.6 ± 1.1	0.0286	42	0.97
N26D, N131D	2.3 ± 0.2	0.0005	21.3 ± 1.3	0.1908	42	0.97
N26D, N131D, N139D	2.8 ± 0.2	0.0670	14.5 ± 0.9	0.0079	42[i]	0.97

[a]Data are shown as mean ± standard error of the mean (SEM) of *N* number of assays. [b]P values are calculated with unpaired *t* test between WT and different mutants. [c]*N* represents the number of replicates of ThT amyloid assays performed for each protein. [d]Unpaired *t* test between N139D and triple mutant yielded $p = 0.5514$ for inverse propagation constant and $p = 0.2263$ for lag time. [e]11.5%. [f]44.1% of replicate experiments did not result in a substantial increase in fluorescence (i.e., appeared flat, resulting in sigmoidal fits with $R^2 < 0.9$) and were not included in calculation of mean lag time or propagation constant. These flat plots are nonetheless shown in Figure S2. [g]Unpaired *t* test between N139D and triple mutant yielded $p = 0.7018$ for inverse propagation constant and $p = 0.3008$ for lag time. [h]12%. [i]21% of replicate experiments did not result in a substantial increase in fluorescence (i.e., appeared flat, resulting in sigmoidal fits with $R^2 < 0.9$) and were not included in calculation of mean lag time or propagation constant. These flat plots are nonetheless shown in Figure S3.

of aggregated SOD1 proteins was confirmed with transmission electron microscopy (Figure 6C).

In the absence of NaCl, the triply deamidated analog of apo-SOD1 exhibited a shorter mean lag time than WT apo-SOD1 by a factor of 1.7 ($p < 0.0001$***) and a smaller mean inverse propagation constant than WT by a factor of 1.6 ($p = 0.0003$) (Table 1). The mean lag time of the triply deamidated analog was, however, indistinguishable from N139D apo-SOD1 in the absence of NaCl ($p = 0.2263$); the mean inverse propagation constants of the triple mutant and N139D were also indistinguishable ($p = 0.5514$). In the presence of 100 mM NaCl, the fibrillization of the triply deamidated analog of apo-SOD1 exhibited a significantly shorter mean lag time than WT apo-SOD1, by a factor of 1.3 ($p = 0.0079$**) (Table 1, Figure 6B). The triple mutant apo-SOD1 protein exhibited a similar mean inverse propagation constant than WT apo-SOD1 ($p = 0.0670$), which suggested that although the fibrillization of the triple mutant initiated earlier than WT apo-SOD1, the rate of propagation of the triple mutant fibrils was identical to WT fibrils, in 100 mM NaCl. Most importantly, the mean inverse propagation constant and mean lag time of the triple mutant were statistically indistinguishable from those of N139D SOD1 ($p = 0.7018$ and 0.3008, respectively, Table 1), suggesting that the N139D ALS variant and triply deamidated apo-SOD1 exhibited identical rates of aggregation in 100 mM NaCl.

We note that 12% of replicate ThT fluorescence plots of N139D (in 0 mM and 100 mM NaCl) and 36% of replicate ThT fluorescence plots of the triply deamidated analog (in 0 mM and 100 mM NaCl) appeared as predominantly flat lines, i.e., exhibited a nearly negligible sigmoidal increase in fluorescence of <2 arbitrary units (from the baseline) throughout the 150 h assay (Figures S2D,E and S3D,E). A sigmoidal fit of these predominantly flat plots, which were only observed during the aggregation of N139D and N26D/N131D/N139D apo-SOD1, yielded R^2 values below 0.9. We, therefore, chose not to incorporate the lag times and inverse propagation constants from these fittings into the calculation of the mean lag time and inverse propagation constants listed in Table 1. A visual inspection of these low-intensity samples at the end of the assay revealed turbidity, which suggested that the SOD1 proteins did indeed aggregate, albeit not into oligomers that bound fluorescent ThT.

We also point out that although the majority of replicate experiments for all proteins exhibited a single predominant sigmoidal increase in ThT fluorescence (denoted τ_1 in Figures S2 and S3), we did observe that ∼15% of the replicates exhibited a second minor sigmoidal increase in fluorescence (denoted τ_2 in Figures S2 and S3). This second transition, which was observed more often in the N139D and N26D/N131D/N139D apo-SOD1 proteins than other proteins, occurred 2−3 days after the first increase in fluorescence. The lag times and inverse propagation constants for this second sigmoidal increase in fluorescence were not incorporated into the calculation of mean lag times and inverse propagation constants listed in Table 1, i.e., this second transition was excluded from all mathematical fittings because of its infrequency of occurrence and minor amplitude. Future studies will be required to determine the cause of this second transition. Additional details of the raw ThT data from the amyloid assays including the shortcomings of the ThT assay and possible causes of variation in fluorescence intensity among fibrils of WT SOD1 and all four variants of SOD1 are discussed further in Supporting Information.

Analysis of WT and mutant SOD1 proteins with ESI-MS, UV−vis, and SDS-PAGE before initiation of the ThT assays demonstrated that all proteins were present at identical concentrations and degrees of purity (Figures 4 and 6D). The centrifugation and SDS-PAGE analysis of the supernatant of SOD1 solutions after completion of the ThT assay demonstrated that the majority (i.e., > 80%) of WT and mutant SOD1 proteins underwent aggregation in 100 mM NaCl (to a sedimentable form) during the 150 h amyloid assay. A small amount of N139D SOD1 (i.e., 3%) and N26D/N131D/N139D SOD1 (i.e., 14%) remained in the supernatant upon completion of the aggregation assay (Figure 6E), which suggests the presence of native (monomeric or dimeric) SOD1 and/or oligomers that were too small to sediment during centrifugation at 13 000 rpm.

dx.doi.org/10.1021/ja407801x | J. Am. Chem. Soc. 2013, 135, 15897−15908

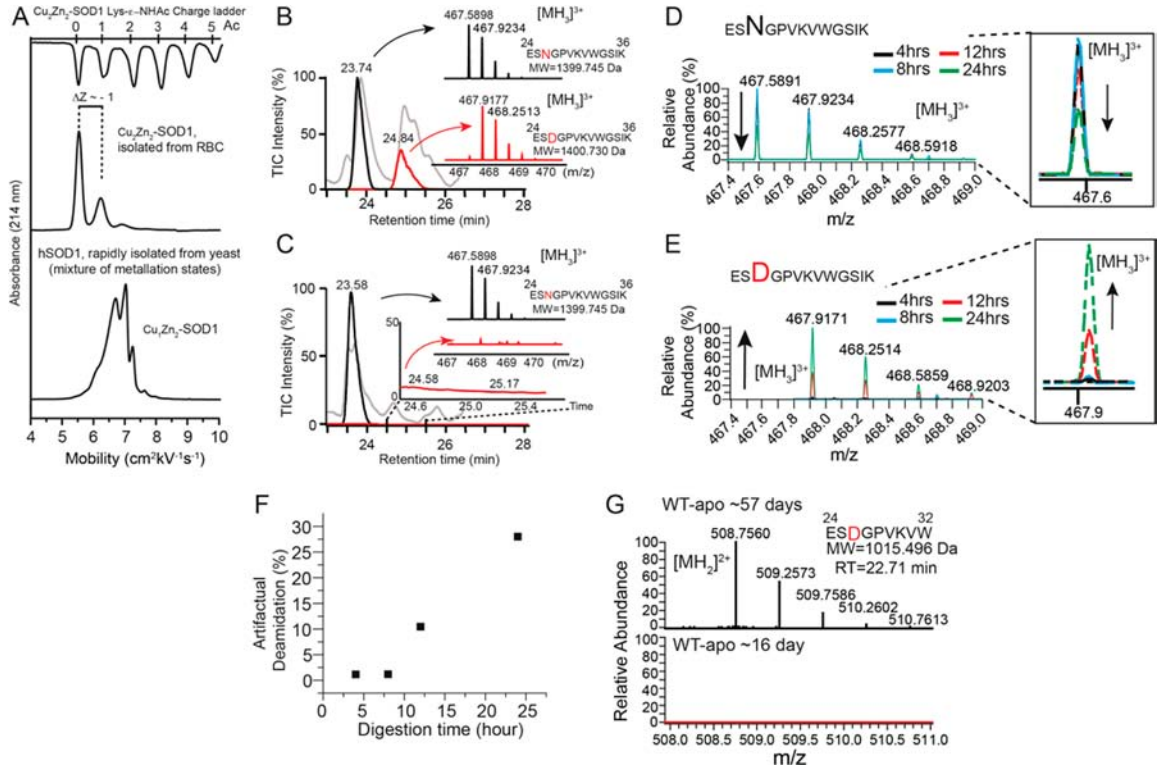

Figure 7. Deamidation of Asn26 is observed in human WT SOD1 isolated from human erythrocytes but not in recombinant WT SOD1 that is freshly isolated from yeast, i.e., that existed in aqueous solution for <13 days prior to analysis (see Materials and Methods for description of time required to express and purify SOD1). (A) Capillary electropherogram of: (top) WT SOD1 from human erythrocytes and (bottom) freshly isolated recombinant human WT SOD1 (with multiple metalation states). A protein charge ladder of holo-SOD1 (from erythrocytes) is inverted to provide a "charge ruler" to estimate the change in charge (ΔZ) of the small satellite peak. (B) Ion extracts from chromatogram of HPLC separation of tryptic digest of SOD1 from erythrocytes (4 h digest); the two ions 467.5898 *m*/*z* (black trace) and 467.9177 (red trace) correspond to the theoretical *m*/*z* of $[MH_3]^{3+}$ of residues 24−36 in WT SOD1 (i.e., ES[N/D]GPVKVWGSIK). Measured mass is listed below amino acid sequence. The gray trace represents raw chromatogram of all eluents. (C) Similar ion extracts (467.5898 *m*/*z*, black trace; 467.9177, red trace) from chromatogram of tryptic digest of "fresh" recombinant human WT SOD1 (4 h digest). The tryptic peptide 24−36 containing D26 is not detected. (D and E) Intensity of mass spectra of tryptic peptide 24−36 (containing Asn26) decreases in intensity (D) while artifactually deamidated peptide 24−36 (with Asp26) increases in intensity (E) during 24 h tryptic digest. (F) Plot of artifactual deamidation of Asn26 (that occurred during proteolysis) as a function of digest time. (G) Top: Deamidation of N26 detected in recombinant WT apo-SOD1 after the protein has existed in solution for ∼60 days. Bottom: deamidation is not detected in the same sample after only ∼16 days in solution.

Asparagine is Deamidated to Aspartate in WT SOD1 Purified from Human Blood. In order to begin to determine if asparagine deamidation occurs to SOD1 in humans and also to establish mass spectrometric protocols (that are free of artifactual deamidation) that can be used by researchers in future studies to search for deamidated SOD1 from tissue extracts, we determined the extent of deamidation in an analytical standard of human SOD1 that is commercially available (from Sigma-Aldrich) as a lyophilized powder. This copper- and zinc-containing form of human SOD1 (denoted holo-SOD1) is isolated from human erythrocytes and has been utilized by dozens of research groups for several decades in clinical and biochemical studies of SOD1 and reactive oxygen species (wherein it is used as an analytical standard in immunohistochemical, electrophoretic, and enzymological studies of SOD1 and reactive oxygen species).[46−61] The deamidation of asparagine has never been reported to occur in this (or any) form of native human SOD1.

We reiterate that our intent in the analysis of this analytical "legacy" standard of SOD1 (Figure 7) was not to necessarily establish (definitively) that asparagine deamidation occurs to SOD1 *in vivo*—collecting such data must be the subject of future studies—but to demonstrate that asparagine deamidation can (if present) remain easily overlooked, even in an analytical standard of SOD1 that has been used for >30 years. Nevertheless, if the deamidation of SOD1 is a physiologically relevant reaction in some human tissues, then we would expect (based upon the Robinson algorithm) to observe the deamidation of the most reactive asparagine in SOD1 proteins isolated from erythrocytes. For example, the SOD1 proteins that are isolated from erythrocytes are expected to have moderately long lifetime because erythrocytes cannot synthesize proteins after erythrogenesis and the lifetime of erythrocytes is ∼120 days.[62,63]

A combination of capillary electrophoresis (which can separate proteins that differ in net charge by as little as a single unit), rapid proteolysis with immobilized trypsin, and LC-ESI-MS/MS was used to detect deamidation at N26 in WT holo-SOD1 from Sigma-Aldrich (as isolated from human erythrocytes) (Figure 7). The electropherogram of holo-SOD1 contained a small satellite peak (μ = 6.14 $cm^2 \cdot kV^{-1} \cdot min^{-1}$) that was consistent with an increase in net negative charge (denoted *Z*) of a single unit, according to alignment with second rung of the Lys-$NHCOCH_3$ "protein charge ladder" of holo-SOD1 (Figure 7A). The protein charge ladder of SOD1, which operates as a "charge ruler", was made by

dx.doi.org/10.1021/ja407801x | J. Am. Chem. Soc. 2013, 135, 15897−15908

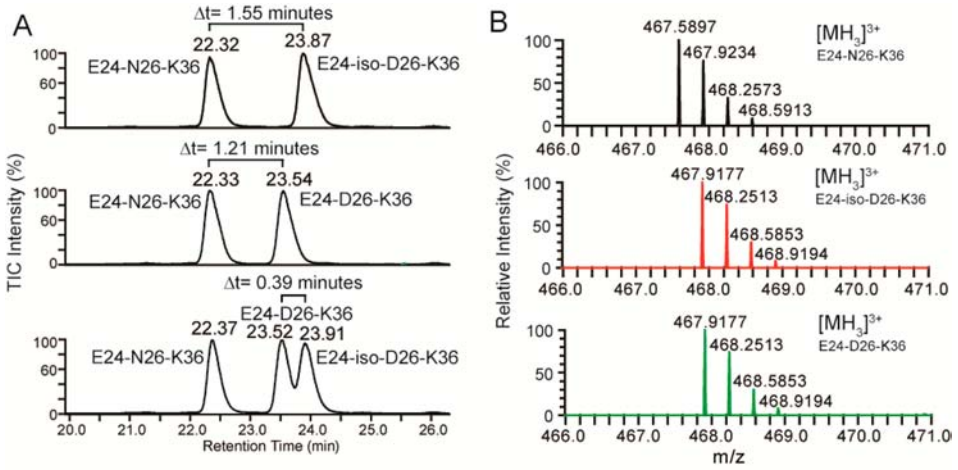

Figure 8. (A) Reversed-phase liquid chromatographs of mixtures of synthetic peptides with identical sequences to residues 24−36 from SOD1, wherein residue 26 contained either: Asn26, Asp26, or iso-Asp26. Top: a mixture of peptides with Asn26 and iso-Asp26; middle: Asn26 and Asp26; and bottom: all three peptides. (B) Mass spectra of peptides from (A). Top: residues 24−36 with Asn26; middle: residues 24−36 with iso-Asp26; bottom: residues 24−36 containing Asp26.

successively acetylating surface Lys-ε-NH_3^+ with acetic anhydride to yield electrostatically neutral Lys-ε-NHAc. Thus, the second "rung" of the charge ladder will be isoelectric with a singly deamidated SOD1 protein. The integration of this satellite peak at μ = 6.14 (which represented deamidated SOD1, as we show below) yielded an intensity that was 24.9% of the major peak. This satellite peak does not represent a different metalation state of SOD1, as demonstrated by its persistence after demetalation (Figure S2).

Rapid trypsinization of human WT holo-SOD1 from human erythrocytes and analysis with HPLC-MS/MS demonstrated that N26 is deamidated to aspartic acid and thus contributes (at least partially) to the intensity of the small satellite peak in the capillary electropherogram in Figure 7A. For example, the tryptic peptide corresponding to residues 24−36, which eluted at t = 23.74 min, was 0.985 Da lower in mass than the tryptic peptide (which also contained residues 24−36) that eluted 1.1 min later at 24.84 (Figure 7B). The MS/MS spectra of the eluting peptides confirmed the presence of N26 in the peptide at 23.74 min and D26 in the peptide at 24.84 min (Figure S3). There were no other deamidated residues detected in WT holo-SOD1 from erythrocytes. The intensity of the peak at 24.84 min representing residues 24−36 with deamidated N26 was 22.4% of the intensity of the peak at 23.74 min, suggesting that 22.4% of the SOD1 protein is deamidated at N26, which is nearly equal to the estimate of 24.9% deamidation from the capillary electropherogram. Quantifying the amount of deamidated N26 from the intensity of mass spectral ions is appropriate when considering experiments, described below, which show that the ionization efficiency of the deamidated and undeamidated peptides is approximately similar (i.e., see similar mass spectral intensity of synthetic peptides; Figure 8A)

The extent of deamidation that we detected at N26 in WT SOD1 from erythrocytes (i.e., ∼23%, based upon the integration of peaks in the chromatogram and electropherogram) is ∼2-fold lower than the theoretical percentage that is predicted from the Robinson algorithm, i.e., ∼50% deamidation, after ∼70 days (Figure 3). This theoretical percentage was inferred by assuming that the SOD1 proteins from Sigma-Aldrich existed in an aqueous (i.e., nonfrozen and non-lyophilized) environment for an average of ∼70 days before analysis with CE and MS. This "age" of SOD1 is based upon the average lifetime of erythrocytes (i.e., ∼ 60 days, assuming a maximum lifetime of ∼120 days) and the time required to purify SOD1. The lyophilized SOD1 protein that is purchased from Sigma-Aldrich requires 9 days to purify from blood samples (which is collected at a private blood bank)[64] utilizing a proprietary protocol that has been used for decades without modification[64] (and is adapted from long-used protocols).[65−67] This proprietary protocol involves lysis, ammonium sulfate precipitation, cation and anion exchange chromatography, and a proprietary thermal denaturation step (which is unique to the method of purification utilized by Sigma-Aldrich but presumably denatures under-metalated SOD1 species and thus results in a high-metal content).[64]

The deamidation of N26 in WT holo-SOD1 from erythrocytes is not an artifact of proteolysis with trypsin or of analysis with LC-MS. For example, we found that artifactual deamidation did occur during proteolysis but could be eliminated by completing trypsin digests in 4−8 h (with immobilized trypsin). Trypsin digests longer than 8 h resulted in detectable artifactual deamidation at N26 (Figure 7E). Moreover, artifactual deamidation was not observed at other Asn residues. The sequence coverage of SOD1 in MS/MS experiments was >95%.

In order to determine if deamidation of N26 can be observed in WT SOD1 shortly after translation, we analyzed recombinant human WT SOD1 immediately after isolating the recombinant human protein from yeast (Figure 7). These recombinant SOD1 proteins had been in aqueous solution for <13 days prior to analysis with CE or MS (i.e., the time required to express, purify, and freeze protein). The electropherogram of "fresh" recombinant SOD1 exhibited a tight clustering of partially resolved peaks that represent a mixture of different metalation states, as demonstrated by the emergence of a single peak after complete demetalation (Figure S2). Deamidation was not detected in any Asn residues in this recombinant WT SOD1 after trypsinization and MS/MS, including at N26 (Figure 7C). Deamidation at N26, but not at any other Asn residue, could be detected in recombinant human WT apo-SOD1 (Figure 7G) after the protein had been incubated in solution for ∼60 days (i.e., 8 days of cell growth, 5

dx.doi.org/10.1021/ja407801x | J. Am. Chem. Soc. 2013, 135, 15897−15908

days of purification, 7 days of demetalation, and 41 days of incubation at pH 7.4, 37 °C); deamidation was not detectable after only 16 days of similar incubation at pH 7.4, 37 °C. We were prevented from quantifying the deamidation in folded SOD1 at $t > 2$ months because of loss of protein signal during CE and ESI-MS (possibly due to protein aggregation or misfolding).

The authenticity of the MS/MS identification of the tryptic peptide containing deamidated N26 was further confirmed by LC-MS/MS analysis of synthetic peptides that were identical to residues 24−36 in WT SOD1 but contained either N26, D26, or iso-D26 (Figure 8). The MS/MS spectra of the peptides derived from proteolysis of SOD1 were identical to synthetic peptides containing N26 and D26 (or iso-D26) (Figure S3). Because our MS/MS instrument does not generate "z" daughter ions, we could not use MS/MS to determine whether N26 deamidated to aspartate or iso-aspartate. Each of the three synthetic peptides were, however, separable with HPLC (Figure 8A), and a comparison of their elution time with elution times of SOD1 peptides allowed us to confirm that N26 deamidated to aspartate in SOD1 and not to iso-aspartate. For example, the Δt_{elute} was 1.6 min for synthetic peptides containing N26 and iso-D26, whereas $\Delta t_{elute} = 1.2$ for synthetic peptides containing N26 and D26 (Figure 8A), which is similar to the $\Delta t_{elute} = 1.1$ observed for the D26 and N26 peptides derived from the proteolysis of WT SOD1 (Figure 7B).

The deamidation of N26 in WT SOD1 to predominantly D26, with no detection of iso-D26, is not in conflict with what (little) is known about the deamidation of Asn in folded proteins. Although previous studies on short disordered peptides have shown that the deamidation of Asn generally favors the formation of iso-Asp over Asp, by a ratio of 3:1,[1,68,69] other studies have shown that the ratio can be inverted in folded proteins to 1:2 in favor of Asp (presumably due to the steric constraints that prevent the reconfiguration of the polypeptide backbone that is required during the formation of iso-Asp).[69] The formation of iso-Asp can also be intrinsically disfavored in some proteins because of specific interactions with nearby residues. For example, the isomerization of Asp15 to iso-Asp15 in the H15D mutant of histidine-containing phosphocarrier protein (HPr) is inhibited by the presence of Glu85; the deletion of Glu85 (via site-directed mutagenesis) allows the interconversion of iso-Asp15 and Asp15.[70] Nevertheless, we cannot rule out the possibility that a significant fraction of N26 in WT SOD1 does deamidate to iso-Asp, but that this isomeric form of SOD1 is lost during protein purification (possibly due to its potential instability) or is present at low abundance and difficult to detect.

Deamidation of Asparagine in SOD1: A Molecular Clock or a Ticking Time Bomb? The presence of the Ser_{25}-Asn_{26}-Gly_{27} motif in a solvent exposed loop of SOD1 appears to predispose N26 to spontaneous deamidation, which suggests that the deamidation of N26 might play a functional role in the cell biology of holo-SOD1 (e.g., in signal transduction). Signal transduction cascades that involve non-enzymatic deamidation (triggered by increases in intracellular pH) have been delineated.[71,72] We do not suspect that the deamidation of N26 is toxic to motor neurons because N26 has not been identified as the site of an ALS-linked missense mutation (as of yet) and the effects upon the structure, stability and aggregation propensity are small. We do not, however, rule out the possibility that the deamidation of N26 is intrinsically toxic because several ALS mutations (e.g., D90A and D101N) are known to have subtle effects on the structure and thermostability of SOD1.[73,74]

Unlike other post-translational chemical modifications to SOD1 (e.g., the oxidation of histidine, tryptophan or cysteine; glycation of lysine; glutathionylation or palmitoylation of cysteine, or the phosphorylation of serine)[19−28] that require the intracellular presence of reactive oxygen species, lipids, enzymes, glycans or other small molecules (at catalytic, stoichiometric, or excessive concentrations), the deamidation of asparagine is a reaction that is mediated by water and hydroxide ion and is thus occurring perennially throughout the lifetime of a protein. The deamidation of asparagine is thus initiated—albeit at different rates depending upon the primary and three-dimensional structure of each asparagine—at the moment of protein translation. The incessant occurrence of non-enzymatic deamidation and the likelihood that the reaction occurs to SOD1 proteins steadily over time suggests to us that the WT SOD1 protein becomes a type of "time bomb" that starts "ticking" at the moment which it is expressed in a motor neuron. This "ticking time bomb" hypothesis implies that the concentration of deamidated SOD1 would be directly proportional to its lifetime and intracellular pH (and possibly the state of metalation, i.e., the loop containing N139 is intrinsically disordered prior to coordinating metal ions and might undergo deamidation more rapidly in the apo-state than holo-state). The "ticking time bomb" hypothesis also suggests that the concentration of deamidated SOD1 would be greater in longer motor neurons than shorter ones, which could offer one (albeit simple) hypothesis for why the longest motor neurons involved in upper or lower limb extremities are the first to be reportedly affected in ALS.[75] We can only speculate on the abundance of N139-deamidated SOD1 that would be required to induce motor neuron death, however, the heterozygous nature of the N139D mutation suggests the level to be ≤50%.

Although this study represents the first detection of asparagine deamidation in intact human SOD1, we suspect that deamidation has been detected in previous 2D electrophoretic studies of SOD1 from cultured cells and neural tissue.[26,31−33] Multiple analyses of WT and ALS mutant SOD1 proteins from human and transgenic mouse tissue[26,31−33] have consistently detected a series of multiple isoforms of human SOD1 with reduced isoelectric points consistent with successive deamidation (i.e., pI = 6.2, 5.9, 5.6, 5.3, and 5.1).[31] Many of these isoforms have identical molecular weights (according to SDS-PAGE) and were not reported to contain chemical modifications according to tandem mass spectrometry.[26] These previous studies did not, however, discuss the possibility of asparagine deamidation, whose formation is not mutually exclusive of other modifications, and we presume that the sub-Dalton modification was not queried during MS/MS peptide fingerprinting (and would be difficult to detect, *de novo*, especially if instrument or search algorithm tolerances for parent or daughter ions were ±1 Da).

■ CONCLUSION

This study demonstrated that the sequential deamidation of N26, N131, and N139 to aspartate can convert the WT SOD1 polypeptide into a pseudo-ALS mutant isoform with a destabilized conformation and accelerated rate of aggregation that is indistinguishable from ALS-linked N139D SOD1. Although this study only examined one particular sequence of compounded deamidation, we do not rule out the possibility (and potential importance) of deamidative reactions that occur

stochastically or in a different sequence than examined in this study. Future studies will need to be performed to determine the extent of asparagine deamidation in human WT SOD1 that is expressed in ALS-affected tissue.

The superoxide dismutase protein is certainly not the first example of a protein whose deamidation accelerates its self-assembly into amyloid-like fibrils. The deamidation of asparagine in amylin and α-synuclein also accelerate their fibrillization into amyloid.[3,76] Moreover, the deamidation or "ticking time bomb" hypothesis that we introduce in this study is by no means limited to cases of ALS that are caused by SOD1. The Asn residues in TDP-43 (which undergoes both anterograde and retrograde transport)[14,77] that are the sites of the recently discovered N378D and N390D ALS mutations are estimated to have even faster intrinsic rates of deamidation than N86 and N139 in SOD1 (as estimated from measured rates of deamidation of pentapeptides with homologous $n + 1$ and $n - 1$ residues).[1] For example, $t_{1/2}$ = 15.1 days for GlySerAsnSerGly (i.e., the peptide analog for N378) and $t_{1/2}$ = 14.9 days for GlySerAsnAlaGly (i.e., the analog N390).[1] The three-dimensional structure of the entire TDP-43 protein has not yet been reported. Thus, we cannot use the Robinson algorithm[4] to predict the rates of deamidation of its 28 Asn residues within its native state. Nevertheless, the fact that mutations in two different ALS-linked genes result in similar Asn-to-Asp substitutions on their gene products raises another hypothesis. The concurrent, collocal deamidation of two (or more) different ALS-linked proteins, e.g., N139 in SOD1 and N378 in TDP-43 might antagonize motor neurons synergistically, thus lowering the concentration of each isoform that would have alone been required for pathogenesis.

MATERIALS AND METHODS

Prediction of Deamidation Rates from the Solution Structure of Human WT holo-SOD1. The rate of deamidation for each Asn residue in folded WT Cu_2Zn_2−SOD1 (PDB: 1L3N) was estimated by Noah C. Robinson (37 °C, pH 7.4, 0.15 M Tris) using a previously developed algorithm.[4]

Purification of SOD1 Proteins. The expression, purification, demetalation, quantitation (of protein and metal stoichiometry), and remetalation of recombinant human WT SOD1 from *Saccharomyces cerevisiae* are described in Supporting Information. The time required to express and purify SOD1 is critical to interpreting the kinetics of deamidation and involved: 8 days of expression (at 30 °C, pH 6.5), 5 days of purification (at room temperature, pH 7.0−8.0), and 7 days of demetalation (4 °C, pH 3.8−5.5). After purification, a portion of the "as-isolated" protein was immediately frozen in order to determine the extent of deamidation in SOD1 immediately after expression and purification. Another aliquot of recombinant SOD1 was demetalated and incubated at 37 °C, pH 7.4 for up to 41 additional days in order to assess deamidation (the solution conditions at which these proteins were incubated included: 5 μM SOD1, 150 mM NaCl, 50 mM KCl, 1 mM dithiothreitol, 5% glycerol, 0.002% sodium azide, 10 mM potassium phosphate).

Capillary Electrophoresis, Differential Scanning Calorimetry, Circular Dichroism, and Amide Hydrogen−Deuterium Exchange of SOD1 Proteins. Preparation of SOD1 protein charge ladders from lyophilized WT holo-SOD1 (isolated from erythrocytes, Sigma-Aldrich) and analysis of all SOD1 proteins with CE were performed as previously described.[78] Differential scanning calorimetry was performed on a Microcal VP-DSC (scan rate = 1 °C/min, 10 mM potassium phosphate, pH 7.4, 2.00 ± 0.03 mg/mL SOD1). Circular dichroism spectroscopy of apo-SOD1 was performed at pH 7.4, 22−23 °C, 15 μM SOD1 (dimer) as previously described.[78] Amide H/D exchange experiments were performed at 22−23 °C, pD 7.4 (10 mM phosphate, 90% D_2O) as previously described.[37] The extent of H/D exchange was quantified with ESI-MS after 5 and 60 min in deuterated buffer. Seven separate H/D exchange experiments were performed for each time point and measured in triplicate (resulting in 21 mass measurements for each protein at each time point). See Supporting Information for additional details.

Thioflavin-T Fluorescence Amyloid Assay. A microplate-based ThT fluorescence assay was used to measure the fibrillization of disulfide-reduced apo-SOD1 proteins (pH 7.4, 37 °C, 60 μM SOD1 monomer) with and without 100 mM NaCl, as previously described (with modifications described in Supporting Information).[44] Data were collected continuously over a period of at least 150 h. In order to determine the lag time and the inverse propagation constant from each ThT aggregation assay, a sigmoidal function was fit to resulting plots, as described in Supporting Information (and illustrated in Figure S1). ThT amyloid assays were carried out for each protein in replicates of between 42 and 96 (depending on availability of protein) so that the statistical significance of average fibrillization rates could be compared among different SOD1 proteins (using an unpaired t test at a 95% confidence interval). After completion of the aggregation assay, aliquots of each SOD1 protein from replicate assays (at least 6) were mixed together and analyzed with transmission electron microscopy to confirm the presence of fibrillar species (see Supporting Information for additional experimental details).

To quantify the extent of aggregation, solutions of SOD1 were also analyzed with denaturing SDS-PAGE (Coomassie staining) prior to initiating the aggregation assay and after completion. Prior to aggregation, 20 μL of soluble protein solutions (60 μM SOD1 monomer) were diluted 2-fold into Lammeli's buffer and analyzed with SDS-PAGE. After aggregation, protein solutions from 6 replicate microplate wells were combined and centrifuged at 13 00 rpm for 30 min. The resulting supernatant was filtered with a syringe filter (0.2 μm), and 20 μL was diluted 2-fold into Laemmli's buffer. All samples were heated to 95 °C for 5 min before loading into gel cassette.

Trypsinization and Mass Spectrometric Analysis of SOD1. Immobilized trypsin (Promega) was used in all digests. An aliquot of each SOD1 solution (100 μL, 178 μM SOD1, 50 mM NH_4HCO_3, pH 7.5) was combined with a slurry of immobilized trypsin (350 μL, 50 mM NH_4HCO_3, pH 7.5) into the filter cup of a centrifugal filtration device (5000 Da cutoff). To this mixture, 4.5 μL of 1 M dithiothreitol (DTT) was added. The digest slurry was incubated at 37 °C for 4 h and analyzed with LC-MS/MS (see Supporting Information for chromatographic details). Identical tryptic digests were also carried out for 8, 12, and 24 h.

Synthetic Peptides Containing Asn26, Asp26, or iso-Asp26. Three synthetic peptides that were identical to the Asn26-containing peptide from trypsin proteolysis of WT SOD1 (i.e., residues 24−36: ESNGPVKVWGSIK) were synthesized, wherein residue 26 was either: Asn, Asp, or iso-Asp. Peptides were synthesized using solid-phase synthesis by New England Peptide (NEP) and received as a lyophilized powder (see Supporting Information for protocols). Each peptide had a molecular weight within 0.1% of the theoretical mass and a purity >98%, according to HPLC and MALDI-TOF mass spectrometry by NEP. Certificates of analysis from NEP are shown in Supporting Information. We also verified the purity and peptide sequence with LC-ESI-MS/MS. The Asn26 peptide was mixed with Asp26 and/or iso-Asp26 peptides in equal concentration (2.0 μM) and analyzed with the same LC-ESI-MS/MS method described for tryptic digests of WT SOD1.

ASSOCIATED CONTENT

Supporting Information

Additional experimental details, additional supporting data, and an expanded discussion of data can be found in Supporting Information, including: (i) the complete set of 534 longitudinal plots of ThT fluorescence for WT, N26D, N131D, N139D, and N26D/N131D/N139D apo-SOD1; (ii) the tandem mass spectra of synthetic peptides and peptide fragments of WT SOD1; and (iii) the certificates of analysis of each synthetic

peptide. This information is available free of charge via the Internet at http://pubs.acs.org.

AUTHOR INFORMATION

Corresponding Author
bryan_shaw@baylor.edu

Notes
The authors declare no competing financial interest.

ACKNOWLEDGMENTS

B.F.S. acknowledges the Department of Defense for financial support (ALS Therapeutic Idea Award, W81XWH-11-1-0790). A.A.M. acknowledges the financial support from the Welch Foundation (C-1743). We also thank Arthur B. Robinson and Noah C. Robinson for calculating theoretical rates of deamidation for WT SOD1.

REFERENCES

(1) Robinson, N. E.; Robinson, A. B. *Molecular Clocks: Deamidation of Asparaginyl and Glutaminyl Residues in Peptides and Proteins*; Althouse Press: Cave Junction, OR, 2004.
(2) Robinson, N. E. *Proc. Natl. Acad. Sci. U.S.A* **2002**, *99*, 5283−5285.
(3) Robinson, N. E.; Robinson, M. L.; Schulze, S. E.; Lai, B. T.; Gray, H. B. *Protein Sci.* **2009**, *18*, 1766−1773.
(4) Robinson, N. E.; Robinson, A. B. *Proc. Natl. Acad. Sci. U.S.A* **2001**, *98*, 4367−4372.
(5) Hooi, M. Y.; Raftery, M. J.; Truscott, R. J. *Invest. Ophthalmol. Visual Sci.* **2012**, *53*, 3554−3561.
(6) Hurtado, P. P.; O'Connor, P. B. *Anal. Chem.* **2012**, *84*, 3017−3025.
(7) Catterall, J. B.; Hsueh, M. F.; Stabler, T. V.; McCudden, C. R.; Bolognesi, M.; Zura, R.; Jordan, J. M.; Renner, J. B.; Feng, S.; Kraus, V. B. *J. Biol. Chem.* **2012**, *287*, 4640−4651.
(8) Robinson, N. E.; Robinson, A. B. *Proc. Natl. Acad. Sci. U.S.A* **2001**, *98*, 944−949.
(9) Bystrom, R.; Andersen, P. M.; Grobner, G.; Oliveberg, M. *J. Biol. Chem.* **2010**, *285*, 19544−19552.
(10) Turner, M. R.; Hardiman, O.; Benatar, M.; Brooks, B. R.; Chio, A.; de Carvalho, M.; Ince, P. G.; Lin, C.; Miller, R. G.; Mitsumoto, H.; Nicholson, G.; Ravits, J.; Shaw, P. J.; Swash, M.; Talbot, K.; Traynor, B. J.; Van den Berg, L. H.; Veldink, J. H.; Vucic, S.; Kiernan, M. C. *Lancet Neurol.* **2013**, *12*, 310−322.
(11) Wegorzewska, I.; Baloh, R. H. *Neurodegener. Dis.* **2011**, *8*, 262−274.
(12) Armakola, M.; Higgins, M. J.; Figley, M. D.; Barmada, S. J.; Scarborough, E. A.; Diaz, Z.; Fang, X.; Shorter, J.; Krogan, N. J.; Finkbeiner, S.; Farese, R. V., Jr.; Gitler, A. D. *Nat. Genet.* **2012**, *44*, 1302−1309.
(13) Watanabe, S.; Kaneko, K.; Yamanaka, K. *J. Biol. Chem.* **2013**, *288*, 3641−3654.
(14) Fallini, C.; Bassell, G. J.; Rossoll, W. *Hum. Mol. Genet.* **2012**, *21*, 3703−3718.
(15) Borchelt, D. R.; Wong, P. C.; Becher, M. W.; Pardo, C. A.; Lee, M. K.; Xu, Z. S.; Thinakaran, G.; Jenkins, N. A.; Copeland, N. G.; Sisodia, S. S.; Cleveland, D. W.; Price, D. L.; Hoffman, P. N. *Neurobiol. Dis.* **1998**, *5*, 27−35.
(16) Roy, S.; Winton, M. J.; Black, M. M.; Trojanowski, J. Q.; Lee, V. M. J. *Neurosci.* **2008**, *28*, 5248−5256.
(17) Valentine, J. S.; Doucette, P. A.; Zittin Potter, S. *Annu. Rev. Biochem.* **2005**, *74*, 563−593.
(18) Graffmo, K. S.; Forsberg, K.; Bergh, J.; Birve, A.; Zetterstrom, P.; Andersen, P. M.; Marklund, S. L.; Brannstrom, T. *Hum. Mol. Genet.* **2013**, *22*, 51−60.
(19) Bosco, D. A.; Morfini, G.; Karabacak, N. M.; Song, Y.; Gros-Louis, F.; Pasinelli, P.; Goolsby, H.; Fontaine, B. A.; Lemay, N.; McKenna-Yasek, D.; Frosch, M. P.; Agar, J. N.; Julien, J. P.; Brady, S. T.; Brown, R. H., Jr. *Nat. Neurosci.* **2010**, *13*, 1396−1403.
(20) Guareschi, S.; Cova, E.; Cereda, C.; Ceroni, M.; Donetti, E.; Bosco, D. A.; Trotti, D.; Pasinelli, P. *Proc. Natl. Acad. Sci. U.S.A* **2012**, *109*, 5074−5079.
(21) Proctor, E. A.; Ding, F.; Dokholyan, N. V. *J. Mol. Biol.* **2011**, *408*, 555−567.
(22) Yamakura, F.; Kawasaki, H. *Biochim. Biophys. Acta* **2010**, *1804*, 318−325.
(23) Wilcox, K. C.; Zhou, L.; Jordon, J. K.; Huang, Y.; Yu, Y.; Redler, R. L.; Chen, X.; Caplow, M.; Dokholyan, N. V. *J. Biol. Chem.* **2009**, *284*, 13940−13947.
(24) Ramirez, D. C.; Gomez-Mejiba, S. E.; Corbett, J. T.; Deterding, L. J.; Tomer, K. B.; Mason, R. P. *Biochem. J.* **2009**, *417*, 341−353.
(25) Furukawa, Y.; O'Halloran, T. V. *Antioxid. Redox. Signal.* **2006**, *8*, 847−867.
(26) Choi, J.; Rees, H. D.; Weintraub, S. T.; Levey, A. I.; Chin, L. S.; Li, L. *J. Biol. Chem.* **2005**, *280*, 11648−11655.
(27) Redler, R. L.; Wilcox, K. C.; Proctor, E. A.; Fee, L.; Caplow, M.; Dokholyan, N. V. *Biochemistry.* **2011**, *50*, 7057−7066.
(28) Antinone, S. E.; Ghadge, G. D.; Lam, T. T.; Wang, L.; Roos, R. P.; Green, W. N. *J. Biol. Chem.* **2013**, *288*, 21606−21617.
(29) Du, Y.; Wang, F.; May, K.; Xu, W.; Liu, H. *Anal. Chem.* **2012**, *84*, 6355−6360.
(30) Shaw, B. F.; Lelie, H. L.; Durazo, A.; Nersissian, A. M.; Xu, G.; Chan, P. K.; Gralla, E. B.; Tiwari, A.; Hayward, L. J.; Borchelt, D. R.; Valentine, J. S.; Whitelegge, J. P. *J. Biol. Chem.* **2008**, *283*, 8340−8350.
(31) Basso, M.; Massignan, T.; Samengo, G.; Cheroni, C.; De Biasi, S.; Salmona, M.; Bendotti, C.; Bonetto, V. *J. Biol. Chem.* **2006**, *281*, 33325−33335.
(32) Basso, M.; Samengo, G.; Nardo, G.; Massignan, T.; D'Alessandro, G.; Tartari, S.; Cantoni, L.; Marino, M.; Cheroni, C.; De Biasi, S.; Giordana, M. T.; Strong, M. J.; Estevez, A. G.; Salmona, M.; Bendotti, C.; Bonetto, V. *PLoS One* **2009**, *4*, e8130.
(33) Li, Q.; Vande Velde, C.; Israelson, A.; Xie, J.; Bailey, A. O.; Dong, M. Q.; Chun, S. J.; Roy, T.; Winer, L.; Yates, J. R.; Capaldi, R. A.; Cleveland, D. W.; Miller, T. M. *Proc. Natl. Acad. Sci. U.S.A* **2010**, *107*, 21146−21151.
(34) Rhoads, T. W.; Williams, J. R.; Lopez, N. I.; Morre, J. T.; Bradford, C. S.; Beckman, J. S. *J. Am. Soc. Mass Spectrom.* **2013**, *24*, 115−124.
(35) Marinkovic, P.; Reuter, M. S.; Brill, M. S.; Godinho, L.; Kerschensteiner, M.; Misgeld, T. *Proc. Natl. Acad. Sci. U.S.A* **2012**, *109*, 4296−4301.
(36) Wang, Q.; Johnson, J. L.; Agar, N. Y.; Agar, J. N. *PLoS Biol.* **2008**, *6*, e170.
(37) Shaw, B. F.; Arthanari, H.; Narovlyansky, M.; Durazo, A.; Frueh, D. P.; Pollastri, M. P.; Lee, A.; Bilgicer, B.; Gygi, S. P.; Wagner, G.; Whitesides, G. M. *J. Am. Chem. Soc.* **2010**, *132*, 17411−17425.
(38) Shaw, B. F.; Durazo, A.; Nersissian, A. M.; Whitelegge, J. P.; Faull, K. F.; Valentine, J. S. *J. Biol. Chem.* **2006**, *281*, 18167−18176.
(39) Rodriguez, J. A.; Valentine, J. S.; Eggers, D. K.; Roe, J. A.; Tiwari, A.; Brown, R. H., Jr.; Hayward, L. J. *J. Biol. Chem.* **2002**, *277*, 15932−15937.
(40) Sandelin, E.; Nordlund, A.; Andersen, P. M.; Marklund, S. S.; Oliveberg, M. *J. Biol. Chem.* **2007**, *282*, 21230−21236.
(41) Chiti, F.; Calamai, M.; Taddei, N.; Stefani, M.; Ramponi, G.; Dobson, C. M. *Proc. Natl. Acad. Sci. U.S.A* **2002**, *99* (Suppl 4), 16419−16426.
(42) Chiti, F.; Dobson, C. M. *Annu. Rev. Biochem.* **2006**, *75*, 333−366.
(43) Chiti, F.; Stefani, M.; Taddei, N.; Ramponi, G.; Dobson, C. M. *Nature* **2003**, *424*, 805−808.
(44) Chattopadhyay, M.; Durazo, A.; Sohn, S. H.; Strong, C. D.; Gralla, E. B.; Whitelegge, J. P.; Valentine, J. S. *Proc. Natl. Acad. Sci. U.S.A* **2008**, *105*, 18663−18668.
(45) Gitlin, I.; Carbeck, J. D.; Whitesides, G. M. *Angew. Chem., Int. Ed. Engl.* **2006**, *45*, 3022−3060.
(46) Nakano, M.; Sugioka, K.; Ushijima, Y.; Goto, T. *Anal. Biochem.* **1986**, *159*, 363−369.

(47) Bass, L. A.; Wang, M.; Welch, M. J.; Anderson, C. J. *Bioconjug. Chem.* **2000**, *11*, 527−532.
(48) Hayashi, F.; Means, T. K.; Luster, A. D. *Blood* **2003**, *102*, 2660−2669.
(49) Polasek, T. M.; Elliot, D. J.; Lewis, B. C.; Miners, J. O. *J Pharmacol. Exp. Ther.* **2004**, *311*, 996−1007.
(50) Auclair, J. R.; Boggio, K. J.; Petsko, G. A.; Ringe, D.; Agar, J. N. *Proc. Natl. Acad. Sci. U.S.A* **2010**, *107*, 21394−21399.
(51) Broering, T. J.; Wang, H.; Boatright, N. K.; Wang, Y.; Baptista, K.; Shayan, G.; Garrity, K. A.; Kayatekin, C.; Bosco, D. A.; Matthews, C. R.; Ambrosino, D. M.; Xu, Z.; Babcock, G. J. *PLoS One* **2013**, *8*, e61210.
(52) Molnar, K. S.; Karabacak, N. M.; Johnson, J. L.; Wang, Q.; Tiwari, A.; Hayward, L. J.; Coales, S. J.; Hamuro, Y.; Agar, J. N. *J. Biol. Chem.* **2009**, *284*, 30965−30973.
(53) Ren, G.; Ma, Z.; Hui, M.; Kudo, L. C.; Hui, K. S.; Karsten, S. L. *Mol. Neurodegener.* **2011**, *6*, 29.
(54) Brotherton, T. E.; Li, Y.; Cooper, D.; Gearing, M.; Julien, J. P.; Rothstein, J. D.; Boylan, K.; Glass, J. D. *Proc. Natl. Acad. Sci. U.S.A* **2012**, *109*, 5505−5510.
(55) Poulose, S. M.; Harris, E. D.; Patil, B. S. *J. Nutr.* **2005**, *135*, 870−877.
(56) Hartman, J. R.; Geller, T.; Yavin, Z.; Bartfeld, D.; Kanner, D.; Aviv, H.; Gorecki, M. *Proc. Natl. Acad. Sci. U.S.A* **1986**, *83*, 7142−7146.
(57) Collins, S. J.; Ruscetti, F. W.; Gallagher, R. E.; Gallo, R. C. *J. Exp. Med.* **1979**, *149*, 969−974.
(58) Nakagawara, A.; Nathan, C. F.; Cohn, Z. A. *J. Clin. Invest.* **1981**, *68*, 1243−1252.
(59) Radomski, M. W.; Palmer, R. M. J.; Moncada, S. *Biochem. Biophys. Res. Commun.* **1987**, *148*, 1482−1489.
(60) Francis, J. W.; Hosler, B. A.; Brown, R. H., Jr.; Fishman, P. S. *J. Biol. Chem.* **1995**, *270*, 15434−15442.
(61) Stone, D.; Lin, P. S.; Kwock, L. *Int. J. Radiat. Biol. Relat. Stud. Phys., Chem. Med.* **1978**, *33*, 393−396.
(62) Eadie, G. S.; Brown, I. W., Jr. *J. Clin. Invest.* **1955**, *34*, 629−636.
(63) D'Alessandro, A.; Righetti, P. G.; Zolla, L. *J. Proteome. Res.* **2010**, *9*, 144−163.
(64) Personal communication, Tom Glendening, Ph.D., Senior Technical Service Scientist at Sigma-Aldrich Inc., St. Lous, MO; July, 20, 2013.
(65) Beyer, W. F., Jr.; Fridovich, I. *Anal. Biochem.* **1987**, *161*, 559−566.
(66) Fridovich, I. *Science* **1978**, *201*, 875−880.
(67) Bannister, J.; Bannister, W.; Wood, E. *Eur. J. Biochem.* **1971**, *18*, 178−186.
(68) Geiger, T.; Clarke, S. *J. Biol. Chem.* **1987**, *262*, 785−794.
(69) Capasso, S.; Balboni, G.; Di Cerbo, P. *Biopolymers* **2000**, *53*, 213−219.
(70) Athmer, L.; Kindrachuk, J.; Georges, F.; Napper, S. *J. Biol. Chem.* **2002**, *277*, 30502−30507.
(71) Zhao, R.; Follows, G. A.; Beer, P. A.; Scott, L. M.; Huntly, B. J.; Green, A. R.; Alexander, D. R. *N. Engl. J. Med.* **2008**, *359*, 2778−2789.
(72) Deverman, B. E.; Cook, B. L.; Manson, S. R.; Niederhoff, R. A.; Langer, E. M.; Rosova, I.; Kulans, L. A.; Fu, X.; Weinberg, J. S.; Heinecke, J. W.; Roth, K. A.; Weintraub, S. J. *Cell.* **2002**, *111*, 51−62.
(73) Rodriguez, J. A.; Shaw, B. F.; Durazo, A.; Sohn, S. H.; Doucette, P. A.; Nersissian, A. M.; Faull, K. F.; Eggers, D. K.; Tiwari, A.; Hayward, L. J.; Valentine, J. S. *Proc. Natl. Acad. Sci. U.S.A* **2005**, *102*, 10516−10521.
(74) Shaw, B. F.; Valentine, J. S. *Trends. Biochem. Sci.* **2007**, *32*, 78−85.
(75) Roche, J. C.; Rojas-Garcia, R.; Scott, K. M.; Scotton, W.; Ellis, C. E.; Burman, R.; Wijesekera, L.; Turner, M. R.; Leigh, P. N.; Shaw, C. E.; Al-Chalabi, A. *Brain* **2012**, *135*, 847−852.
(76) Dunkelberger, E. B.; Buchanan, L. E.; Marek, P.; Cao, P.; Raleigh, D. P.; Zanni, M. T. *J. Am. Chem. Soc.* **2012**, *134*, 12658−12667.
(77) Gendron, T. F.; Josephs, K. A.; Petrucelli, L. *Neuropathol. Appl. Neurobiol.* **2010**, *36*, 97−112.
(78) Shi, Y.; Mowery, R. A.; Ashley, J.; Hentz, M.; Ramirez, A. J.; Bilgicer, B.; Slunt-Brown, H.; Borchelt, D. R.; Shaw, B. F. *Protein Sci.* **2012**, *21*, 1197−1209.